Immunity, Vol. 17, 713–723, December, 2002, Copyright ©2002 by Cell Press

Complement Receptors CD21/35 Link Innate and Protective Immunity during *Streptococcus pneumoniae* Infection by Regulating IgG3 Antibody Responses

Karen M. Haas,[1,6] Minoru Hasegawa,[1,6] Douglas A. Steeber,[1] Jonathan C. Poe,[1] Mark D. Zabel,[2] Cheryl B. Bock,[1] David R. Karp,[3] David E. Briles,[4] John H. Weis,[2] and Thomas F. Tedder[1,5]

[1]Department of Immunology
Duke University Medical Center
Durham, North Carolina 27710

[2]Department of Pathology
University of Utah
Salt Lake City, Utah 84132

[3]Department of Internal Medicine
University of Texas Southwestern Medical Center
Dallas, Texas 75390

[4]Department of Cell and Molecular Biology
University of Alabama at Birmingham
Birmingham, Alabama 35294

Summary

The CD21/35 receptor provides an important link between innate and adaptive immunity. Its importance during protective immune responses to encapsulated extracellular bacteria was assessed using a new line of mice completely deficient in CD21/35 expression (CD21/35$^{-/-}$). CD21/35 expression was essential for the rapid trapping of C3dg-antigen complexes by B cells in vivo, especially in splenic marginal zones. Despite normal B cell development in CD21/35$^{-/-}$ mice, T cell-independent and -dependent antibody responses to low-dose antigens were significantly decreased, with a striking impairment in IgG3 responses. Accordingly, CD21/35$^{-/-}$ mice were more susceptible to acute lethal *Streptococcus pneumoniae* infection. Thus, CD21/35 expression is critical for early protective antibody responses to lethal pathogens that rapidly multiply and quickly overwhelm the immune system.

Introduction

Protection against extracellular bacterial infections relies on complex and overlapping interactions between innate and adaptive immune responses. Innate protection includes complement activation since complement-deficient patients are susceptible to infections with encapsulated bacteria such as *Streptococcus pneumoniae,* the predominant cause of community-acquired pneumonias, septicemia, otitis media, and meningitis (Burman et al., 1985; Figueroa and Densen, 1991). The C3 complement component is particularly important for the efficient opsonization, lysis, and clearance of bacteria (Botto and Walport, 1993; Winkelstein, 1981). Administration of cobra venom factor (CVF), a convertase analog that depletes C3, leads to impaired opsonization and clearance of *S. pneumoniae* by anticapsular antibody (Brown et al., 1981). Furthermore, C3-deficient (C3$^{-/-}$) mice have impaired clearance of *S. pneumoniae* (Circolo et al., 1999). The decoration of pathogen-derived antigens with C3 breakdown fragments, C3b, iC3b, and C3d provides signals important for the opsonization or destruction of bacteria by phagocytic and nonphagocytic cells bearing appropriate receptors.

Depletion of C3 in mice by CVF or anti-C3 antibody administration reduces T cell-dependent (TD) and some T cell-independent (TI) antibody responses (Pepys, 1974). Similar defects in humoral immune responses are found in patients with genetic deficiencies in C3 (Bitter-Suermann and Burger, 1989). In addition, C3$^{-/-}$ and C4-deficient (C4$^{-/-}$) mice generate reduced TD antibody responses (Fischer et al., 1996; Wessels et al., 1995), and C3$^{-/-}$ mice have reduced TI antibody responses (Guinamard et al., 2000; Ochsenbein et al., 1999). C3 cleavage products such as C3d form covalent bonds with foreign antigens or pathogens and thereby provide ligands for leukocyte complement receptors 1 (CR1, CD35) and 2 (CR2, CD21). Human CD21 and CD35 are encoded by distinct genes, while mouse CD21 and CD35 are alternatively spliced products of the same *Cr2* gene (Fearon and Carroll, 2000). In mice, CD35 is generated by the addition of six short consensus repeat units (SCRs) to the amino terminal end of the CD21 protein composed of 15–16 SCRs. Thus, in mice, CD35 serves as a receptor for C4b and C3b as well as the CD21 ligands, C3d and iC3b (Fearon and Carroll, 2000). CD21/35 is expressed primarily by mature B cells and follicular dendritic cells where it associates with CD19, a member of the immunoglobulin (Ig) superfamily that functions as a response regulator of transmembrane signals during B cell activation (Poe et al., 2001). CD21/35 plays an important role in enhancing TD antibody responses as treatment with either anti-CD21 mAb (Heyman et al., 1990; Thyphronitis et al., 1991) or soluble receptor (Hebell et al., 1991) impairs humoral immune responses.

Mice with a genetically disrupted *Cr2* locus generate modest TD antibody responses to challenge with low-dose antigens (Ahearn et al., 1996; Molina et al., 1996) but generate near normal primary responses to high-dose TD antigens, antigen/adjuvant challenge, or during secondary responses (Chen et al., 2000; Hasegawa et al., 2001; Molina et al., 1996; Wu et al., 2000). By contrast, the role of CD21/CD35 in TI antibody responses is unknown except that protective TI antiviral antibody responses depend on C3 but not CD21/CD35 expression (Ochsenbein et al., 1999). However, this discrepancy may be explained by the finding that the CD21/35-deficient mouse line used for those experiments (Ahearn et al., 1996) expresses a hypomorphic cell surface CD21/35 protein (Hasegawa et al., 2001). In these mice, splicing-out of the gene-targeted exon in the *Cr2* locus results in a smaller cell surface CD21/35 protein (CD21/35^{hypo}) expressed at ~40% of wild-type levels that may retain ligand binding activity. Therefore, a mouse line completely deficient in CD21/35 expression was gener-

[5]Correspondence: thomas.tedder@duke.edu
[6]These authors contributed equally to this work.

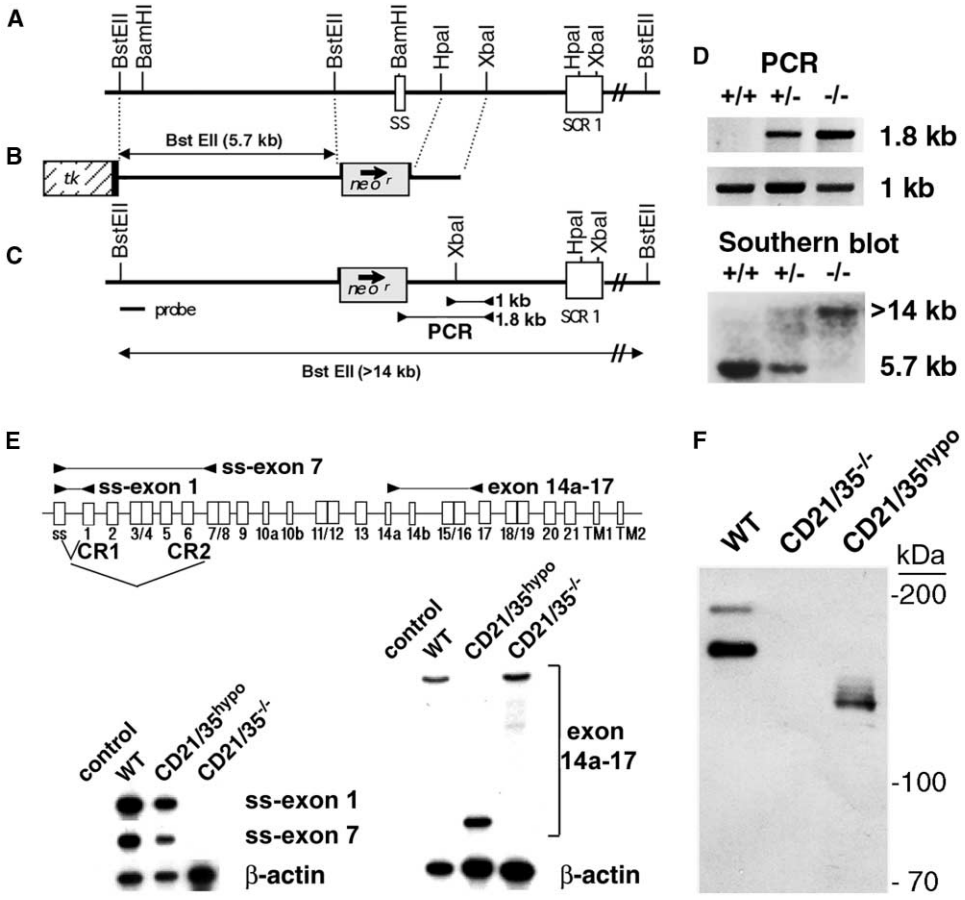

Figure 1. CD21/35$^{-/-}$ Mouse Generation by Targeted Disruption of the *Cr2* Gene

(A) Restriction map of the region of the *Cr2* gene targeted. Signal sequence (SS) and SCR domains are indicated.

(B) The *Cr2* targeting vector showing the location of the thymidine kinase (*tk*) and neomycin-resistance (*neo*^{r}) genes. Genomic DNA between BstEII and HpaI restriction sites including the signal sequence was replaced with the *neo*^{r} gene in the 5′ to 3′ orientation. Blunt end ligations resulted in loss of a BstEII, HpaI, and XbaI site in the targeting construct.

(C) Predicted restriction map of the targeted allele. Homologous recombination increases the BstEII cleavage product from 5.7 to >14 kb.

(D) PCR and Southern blot analysis of genomic DNA from wild-type, CD21/35$^{+/-}$, and CD21/35$^{-/-}$ littermates. PCR amplification used a 3′ primer outside of the targeted region in combination with either a neo-specific primer or control primer specific for the 3′ flanking sequence (as indicated in [C]) to yield PCR products that were 1.8 and 1 kb size, respectively. Southern blot analysis was conducted using BstEII digestion and a probe specific for the 5′ flanking sequence as diagrammed in (C).

(E) Spleen *Cr2* mRNA transcripts in wild-type (WT), CD21/35^{hypo}, and CD21/35$^{-/-}$ mice. PCR products were amplified using the primer sets indicated. β-actin primers and a water blank were included as controls.

(F) Western blot analysis of CD21/35 protein expression in purified spleen B cell lysate from CD21/35$^{-/-}$, CD21/35^{hypo}, and wild-type mice using CD21/35-specific polyclonal antisera (D-19).

ated in the current study to assess the importance of CD21/35 function during responses to TI antigens and foreign pathogens that rapidly multiply and may quickly overwhelm the immune system. The complete genetic disruption of CD21/35 expression had only modest effects on B cell development but revealed a pivotal role for CD21/35 in establishing protective immunity against lethal *S. pneumoniae* infection.

Results

Generation of CD21/35$^{-/-}$ Mice

CD21/35$^{-/-}$ mice were generated using a targeting construct with the 5′ promoter region of the *Cr2* gene deleted (Figure 1). Homologous recombination in embryonic stem cells replaced the *Cr2* promoter region and exon encoding the transcription initiation and signal sequence of the CD21/35 protein product with a Neomycin resistance (*neo*^{r}) cassette that terminated translation (Figures 1A–1C). Chimeric mice resulting from two targeted ES clones were used to generate two independent CD21/35$^{-/-}$ mouse lines with transmission of the mutation verified by Southern blot and PCR analysis (Figure 1D). Mice heterozygous for the targeted allele were mated to generate wild-type, CD21/35$^{+/-}$, and CD21/35$^{-/-}$ littermates at the expected Mendelian frequency. No phenotypic or functional differences were observed between individual CD21/35$^{-/-}$ mouse lines, so the results from only one CD21/35$^{-/-}$ mouse line are described.

Disrupted *Cr2* gene transcription was confirmed by PCR analysis of transcripts produced in spleens of wild-

type and CD21/35$^{-/-}$ littermates in comparison with results from CD21/35^{hypo} splenocytes (Ahearn et al., 1996). Signal sequence encoding transcripts were found in wild-type and CD21/35^{hypo} mice but not in CD21/35$^{-/-}$ mice (Figure 1E, ss-exon 1 and ss-exon 7 PCR products). Transcripts downstream of the targeted signal sequence were detected in CD21/35$^{-/-}$ mice (Figure 1E, exons 14a-17 PCR product), suggesting alternative transcription start sites in the *Cr2* locus or the generation of transcripts extending beyond the *Neo* insertion site. Nonetheless, purified splenic B cells from CD21/35$^{-/-}$ mice did not express detectable CD21/35 protein in Western blot assays using antibodies reactive with the amino or carboxyl terminus of CD21/35 (Figure 1F and data not shown). By contrast, CD21/35^{hypo} mice expressed a shorter CD21/35 protein (Figure 1F) reflecting transcripts lacking exons 15/16 (Figure 1E) that were produced at 30% of wild-type levels in CD21/35^{hypo} mice as determined by real-time PCR analysis (data not shown). Thus, the CD21/35$^{-/-}$ mice described in this study did not express detectable CD21/35 protein.

CD21/35 Function in CD21/35$^{-/-}$ Mice

Cell-surface CD21/35 expression was not detected on cells from CD21/35$^{-/-}$ mice using the CD21/35-specific antibodies, 7G6 and 7E9 (Figure 2A). Similarly, lymphocytes from CD21/35$^{-/-}$ mice failed to effectively bind C3dg-streptavidin-phycoerythrin (C3dg-SA-PE) tetramers (Figures 2B and 2C), which are used to visualize CD21 ligand binding (Henson et al., 2001). By contrast, B cells from CD21/35^{hypo} mice expressed cell surface CD21/35 at ~40% of the density found on B cells from wild-type littermates and bound C3dg-SA-PE complexes (Figures 2A–2C). Blood and spleen B220^{+} lymphocytes from wild-type mice also bound C3dg-SA-PE complexes efficiently compared with nonspecific chicken-γ globulin (CGG)-SA-PE control complexes (Figures 2B and 2C). Thus, CD21/35$^{-/-}$ B cells did not express functional CD21/35 protein, while B cells from CD21/35^{hypo} mice expressed CD21/35 that specifically bound C3dg complexes.

The contribution of CD21/35 function to C3dg-complex binding in vivo was assessed by intravenously administering C3dg-SA-PE or CGG-SA-PE control complexes in CD21/35$^{-/-}$ or wild-type littermates. Thirty minutes following injection, C3dg-SA-PE complexes failed to localize in the splenic marginal zones of CD21/35$^{-/-}$ mice but efficiently decorated the marginal zones of wild-type mice (Figure 2D). Trapping of CGG-SA-PE complexes in either CD21/35$^{-/-}$ or wild-type mice was modest compared with C3dg-SA-PE localization in wild-type mice. Furthermore, splenic B220^{+} B cells isolated from CD21/35$^{-/-}$ mice injected with complexes did not bind C3dg- or CGG-tetramers as visualized by flow cytometry analysis (Figure 2E). By contrast, a significant percentage of B cells from wild-type mice injected with complexes demonstrated measurable C3dg-tetramer binding and modest binding of CGG-SA-PE control complexes (Figure 2E). Thus, CD21/35 expression is critical for the rapid trapping of C3dg-antigen complexes in vivo, especially in splenic marginal zones. Furthermore, CD21/35 expression allows the efficient cell surface localization of C3dg-complexes on a substantial fraction of B cells, independent of their antigen-receptor specificity.

B Cell Development in CD21/35$^{-/-}$ Mice

CD21/35$^{-/-}$ mice had normal frequencies of B220^{lo}CD43^{+} pro-B cells, IgM^{-}B220^{lo} pro/pre-B cells, and B220^{lo}IgM^{+} immature and B220^{hi}IgM^{+} mature B cells in the bone marrow (Table 1). Similarly, blood, spleen, Peyer's patch, lymph node, and peritoneal B cell numbers and frequencies were similar between CD21/35$^{+/+}$, CD21/35$^{+/-}$, and CD21/35$^{-/-}$ littermates. Peritoneal B1 (B220^{+}CD11b^{+}), B1a (B220^{lo}CD5^{+}; CD11b^{+}CD5^{+}), and B-2 plus B1b (B220^{+}CD5^{-}) B cell frequencies and numbers were also similar for CD21/35$^{-/-}$ and wild-type littermates (Table 1 and Figure 2F). Although no significant differences were detected in the frequency or absolute numbers of splenic B220^{+}IgM^{+} B cells, there were differences in B cell subsets as determined by IgM and IgD expression levels. Specifically, the IgM^{hi}IgD^{lo} B cell population constituting marginal zone, B1, and immature transitional 1 (T1) B cells (Loder et al., 1999) was significantly expanded in CD21/35$^{-/-}$ mice, while the IgM^{lo}IgD^{hi} population constituting follicular and mantle zone B cells (Loder et al., 1999) was significantly decreased compared to wild-type littermates (Table 1 and Figure 2G). Spleen marginal zones were well developed in CD21/35$^{-/-}$ mice as assessed by IgM/PNA as well as IgM/IgD immunohistochemical staining (Figure 3A and data not shown), and differences in the frequency of splenic B1a (CD5^{+}IgM^{hi}IgD^{lo}) cells were not found in CD21/35$^{-/-}$ mice (data not shown). Therefore, the expanded population of IgM^{hi} splenocytes in CD21/35$^{-/-}$ mice most likely represents marginal zone B cells.

CD19 Expression by CD21/35$^{-/-}$ B Cells

Since CD21/35^{hypo} B cells express CD19 at ~30% higher density (Hasegawa et al., 2001), B cells from CD21/35$^{-/-}$ mice were similarly examined for altered CD19 expression. Although immature B220^{lo} bone marrow B cells from CD21/35$^{-/-}$ mice expressed CD19 at normal levels (91 $\pm$ 8% of wild-type), CD21/35$^{-/-}$ blood (133 $\pm$ 3%), spleen (148 $\pm$ 13%), lymph node (149 $\pm$ 9%), and peritoneal CD5^{-} B cells (139 $\pm$ 7%), all expressed significantly higher levels of CD19 compared to wild-type littermates (Figure 2H; $n = 5–7$, $p < 0.05$). Peritoneal CD5^{+} B cells, which express low levels of CD21/35, had negligible increases in CD19 expression in the absence of CD21/35 expression (109 $\pm$ 3%, $n = 5$; Figure 2H). Intermediate increases in CD19 expression were observed for CD21/35$^{+/-}$ B cells. These findings demonstrate a direct inverse relationship between CD21/35 expression and CD19 density on the cell surface. Although overall IgM expression was increased on splenic CD21/35$^{-/-}$ B cells, this was mainly due to a decrease in the IgM^{lo}IgD^{hi} population and increase in the IgM^{hi}IgD^{lo} population (Figure 2G). Significant alterations in IgM expression were not found for B cells from blood, Peyer's patches, or lymph nodes of CD21/35$^{-/-}$ mice.

Impaired Humoral Immune Responses in CD21/35$^{-/-}$ Mice

Serum IgM, IgG1, IgG2b, and IgG3 levels were significantly reduced in 2-month-old CD21/35$^{-/-}$ littermates,

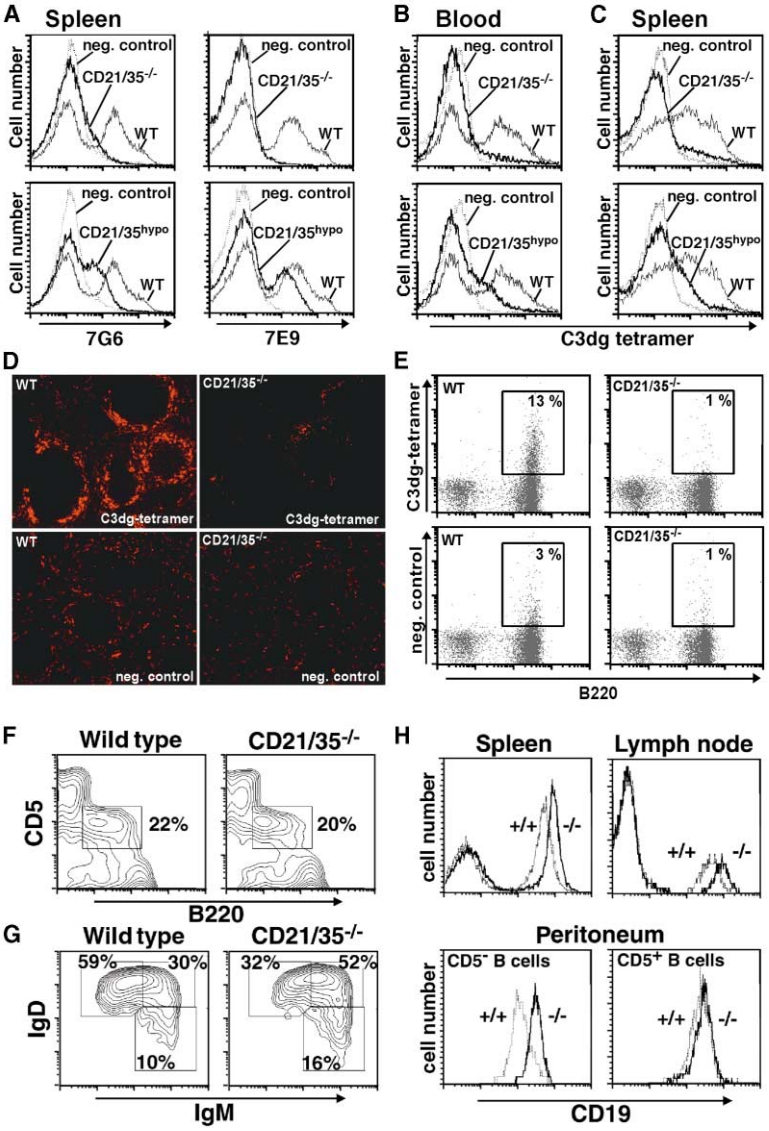

Figure 2. Cell-Surface CD21/35 Expression and Ligand Binding

(A) Splenocytes isolated from CD21/35$^{-/-}$ and wild-type littermates, or CD21/35^{hypo} mice were stained in parallel using 7G6 or 7E9 antibodies and analyzed by flow cytometry. Results are shown for CD21/35$^{-/-}$ (thick line, upper panels), CD21/35^{hypo} (thick line, lower panels), and wild-type (thin line) splenocytes. Dotted lines indicate isotype control staining.

(B and C) C3dg-tetramer binding by blood (B) and spleen (C) lymphocytes from wild-type (thin line), CD21/35$^{-/-}$ (thick line, upper panels), and CD21/35^{hypo} mice (thick line, lower panels) as assessed by flow cytometry. Biotinylated CGG complexed to SA-PE served as a negative control (dotted line).

(D and E) Binding of C3dg-SA-PE complexes in vivo by CD21/35$^{-/-}$ and wild-type littermates. Mice were injected i.v. with 40 μg C3dg-SA-PE or CGG-SA-PE complexes and sacrificed 30 min later. (D) Visualization of C3dg-SA-PE complex trapping in spleen sections by fluorescence microscopy (original magnification, 200×). (E) Binding of C3dg-SA-PE to splenic B cells. Single-cell suspensions of spleens harvested from mice injected with either C3dg-SA-PE or CGG-SA-PE control complexes were stained with B220-FITC and analyzed by flow cytometry. The percentage of cells binding complexes in vivo is indicated.

(F–H) Phenotypic characteristics of CD21/35$^{-/-}$ mice. (F) Normal peritoneal B1a (B220^{lo}CD5^{+}) B cell frequencies in CD21/35$^{-/-}$ mice as determined by B220 and CD5 staining of lymphocyte-gated populations. (G) IgM^{hi}IgD^{lo} B cell subsets are increased, and IgM^{lo}IgD^{hi} B cell subsets are decreased in spleens of CD21/35$^{-/-}$ mice as assessed by flow cytometry. The percentages of B220^{+}-gated cells falling within the IgM^{lo}IgD^{hi}, IgM^{hi}IgD^{hi}, and IgM^{hi}IgD^{lo} gated areas are shown. (H) Increased CD19 density on the surface of CD21/35$^{-/-}$ B cells. Spleen, lymph node, or peritoneal cells of wild-type (+/+) and CD21/35$^{-/-}$ (−/−) mice were stained using an anti-CD19 mAb with flow cytometry analysis. Peritoneal cells were also stained for CD5, with CD19 expression shown for the CD5^{-}/CD19^{+} and CD5^{+}/CD19^{+} lymphocyte-gated subpopulations.

while IgG2a and IgA levels were normal (Figure 3D). Heterozygous CD21/35$^{+/-}$ mice had intermediate serum Ig levels. In agreement with these findings, the frequency of spleen germinal centers (GCs) in naive CD21/35$^{-/-}$ mice was significantly lower than in wild-type littermates ($10 \pm 3\%$ versus $33 \pm 3\%$; $p < 0.01$). However, established GCs in naive CD21/35$^{-/-}$ mice were similar in size to wild-type GCs (Figure 3A). Thus, CD21/35 is important for initiating GC development and promoting normal serum antibody production.

Consistent with reduced serum Ig levels, CD21/35$^{-/-}$ mice had defective antibody responses to TI-1 (TNP-LPS), TI-2 (DNP-Ficoll), and TD antigens (sheep red blood cells [SRBC] and DNP-KLH precipitated in alum) that varied depending on the amount of antigen challenge and antibody isotype being assessed. CD21/35$^{-/-}$ mice generated normal hapten-specific IgM responses to TNP-LPS, near-normal IgM responses to TNP-Ficoll, and normal IgM responses to high-dose SRBC and DNP-KLH challenge (Figure 4). By contrast, IgM antibody responses of CD21/35$^{-/-}$ mice were significantly lower during primary responses to low-dose (5×10^5) SRBC challenge, although normal IgM responses were induced with secondary challenge (Figure 4C). Early hapten-specific IgG antibody responses in CD21/35$^{-/-}$ mice were significantly decreased following TNP-LPS and DNP-Ficoll immunizations (Figures 4A and 4B). Significantly reduced primary and secondary IgG antibody responses were also observed in CD21/35$^{-/-}$ mice following low-dose SRBC challenge (Figure 4C). However, normal IgG responses were observed with high-dose SRBC challenge and with DNP-KLH immunization, especially during secondary responses. Nonetheless, IgG3 antibody responses to both TI and TD antigens were

Table 1. Frequency and Numbers of B Lymphocytes in CD21/35$^{-/-}$ Mice

Tissue	Phenotype	Percentage of Lymphocytes[a]			Number of Cells ($\times 10^{-5}$)[b]		
		Wild-Type	CD21/35$^{+/-}$	CD21/35$^{-/-}$	Wild-Type	CD21/35$^{+/-}$	CD21/35$^{-/-}$
Bone Marrow	B220^{lo}CD43^{+}	12 ± 2	12 ± 1	13 ± 2			
	B220^{lo}IgM^{-}	38 ± 5	37 ± 3	35 ± 2			
	B220^{lo}IgM^{+}	19 ± 1	22 ± 2	20 ± 2			
	B220^{hi}IgM^{+}	14 ± 2	16 ± 1	15 ± 1			
Blood	B220^{+}	44 ± 3	44 ± 3	43 ± 3	18 ± 3	22 ± 5	17 ± 4
Peyer's patches	B220^{+}	71 ± 4	76 ± 3	72 ± 4	24 ± 6	25 ± 3	17 ± 4
Lymph nodes	B220^{+}IgM^{+}	14 ± 3	12 ± 2	15 ± 3	1.1 + 0.2	2.4 + 0.7	1.8 ± 0.6
Spleen	B220^{+}IgM^{+}	54 ± 4	55 ± 5	54 ± 5	280 ± 20	300 ± 50	280 ± 30
	IgM^{lo}IgD^{hi}	26 ± 2	23 ± 2	18 ± 2*	140 ± 10	120 ± 20	96 ± 10*
	IgM^{hi}IgD^{lo}	6.4 ± 0.6	7.0 ± 0.5	8.3 ± 0.4*	31 ± 1	39 ± 7	39 ± 3*
	IgM^{hi}IgD^{hi}	18 ± 2	20 ± 3	24 ± 5	88 ± 12	100 ± 20	120 ± 20
Peritoneum	IgM^{+}	45 ± 4	55 ± 7	51 ± 6	7 ± 2	8 ± 2	9 ± 4
	B220^{lo}CD5^{+}	23 ± 4	25 ± 5	24 ± 4	3 ± 1	3 ± 1	4 ± 2
	B220^{+} CD5^{-}	29 ± 3	26 ± 4	30 ± 4	4 ± 1	4 ± 1	6 ± 3
	B220^{+} CD11b^{-}	5.0 ± 1.3	4.3 ± 0.7	5.7 ± 2.3	0.7 ± 0.4	0.4 ± 0.1	0.6 ± 0.4
	B220^{+} CD11b^{+}	46 ± 5	45 ± 8	47 ± 5	6 ± 2	6 ± 2	8 ± 4
	CD11b^{+} CD5^{+}	23 ± 4	26 ± 5	24 ± 4	3 ± 1	4 ± 1	4 ± 2

[a] Values represent the mean frequency (± SEM) of lymphocytes expressing the indicated surface markers as determined by immunofluorescence staining with flow cytometry analysis. Results were from five to eight mice of each genotype.

[b] Mean B cell numbers (± SEM) were calculated based on the total number of cells harvested from each tissue. For blood, values indicate numbers of cells per ml.

* The percentage or number of cells was significantly different from that of wild-type littermates, $p < 0.05$.

severely impaired in CD21/35$^{-/-}$ mice. For example, IgG3 titers in pooled sera from CD21/35$^{-/-}$ mice were reduced by >90% in response to haptenated TI-antigens or high- and low-dose DNP-KLH (data not shown). Heterozygous littermates produced intermediate to normal levels of antigen-specific IgG3.

The frequency of GCs in follicles of CD21/35$^{-/-}$ mice was significantly reduced during responses to low- and high-dose SRBC challenge (CD21/35$^{-/-}$ versus wild-type: 44 ± 6% versus 61 ± 4%, low dose, and 46 ± 3% versus 67 ± 3%, high dose; both $p < 0.05$). Low-dose DNP-KLH challenge induced 65% fewer GCs in CD21/35$^{-/-}$ mice (21 ± 8% versus 60 ± 5%, $p < 0.01$), while GC formation was normal in CD21/35$^{-/-}$ mice receiving high-dose DNP-KLH (55 ± 6% versus 48 ± 7%). Despite reduced antibody production and lower frequencies of GCs, immunization-induced increases in GC frequencies were proportional between CD21/35$^{-/-}$ and wild-type littermates. In addition, the sizes of GCs in CD21/35$^{-/-}$ mice were not markedly different from those found in wild-type littermates (Figures 3B and 3C). Therefore, CD21/35$^{-/-}$ mice had defective antibody responses to low-dose antigen challenge with a striking failure to generate significant IgG3 antibody responses, even in response to high-dose antigens.

Impaired Protective Immunity to *S. pneumoniae* Infection in CD21/35$^{-/-}$ Mice

Since early antibody responses, especially those of the IgG3 isotype, play a critical role in host defense to extracellular encapsulated bacteria, CD21/35$^{-/-}$ and wild-type littermates were challenged with graded doses of virulent *S. pneumoniae*, strain WU-2. The rate of mortality was similar between CD21/35$^{-/-}$ mice and their wild-type littermates with an LD_{50} between 100–1000 colony forming units (cfu) of bacteria (Figure 5A). Thus, early innate responses required to survive *S. pneumoniae* infection in the absence of previous exposure were comparable between CD21/35$^{-/-}$ and wild-type mice. Nonetheless, CD21/35 expression contributed to the generation of protective immunity against *S. pneumoniae* infection in littermates surviving challenge with 10–100 cfu of live bacteria. Previous infection with live bacteria at 10–100 cfu provided no protection to CD21/35$^{-/-}$ mice rechallenged with a lethal 5000 cfu dose of *S. pneumoniae* 10 days later, while wild-type littermates were protected (40%–67% survival; Figure 5B; pooled results, $p < 0.05$). To test whether immunization with heat-killed bacteria protected against lethal challenge, mice were immunized with graded doses of heat-killed bacteria and challenged 10 days later with 5000 cfu of *S. pneumoniae*. Immunization with 10^3 heat-killed WU-2 did not protect against a lethal dose of *S. pneumoniae* in CD21/35$^{-/-}$ or wild-type littermates (Figure 5C). However, immunization with a 100-fold higher dose of heat-killed bacteria (10^5) provided complete protection in wild-type littermates, but provided CD21/35$^{-/-}$ mice with only partial protection (33% survival) ($p < 0.05$, Figure 5D). Immunization and boosting of mice on day 14 with 10^5 heat-killed bacteria protected all mice against lethal challenge (Figure 5E), as did a single immunization with 10^7 heat-killed bacteria (Figure 5F). Thus, CD21/35 plays a pivotal role in establishing a threshold of protective immunity against lethal *S. pneumoniae* infection.

Reduced protection against infection in CD21/35$^{-/-}$ mice correlated with low bacteria-specific antibody titers. Preimmunization titers of natural antibody reactive with intact *S. pneumoniae* were significantly lower in CD21/35$^{-/-}$ mice than in wild-type littermates (100 ± 20 versus 210 ± 20, respectively, $p < 0.01$; Figure 6A). Ten days following immunization with 10^5 heat-killed bacteria, WU-2-specific antibody titers were nearly 5-fold less in CD21/35$^{-/-}$ mice than in wild-type lit-

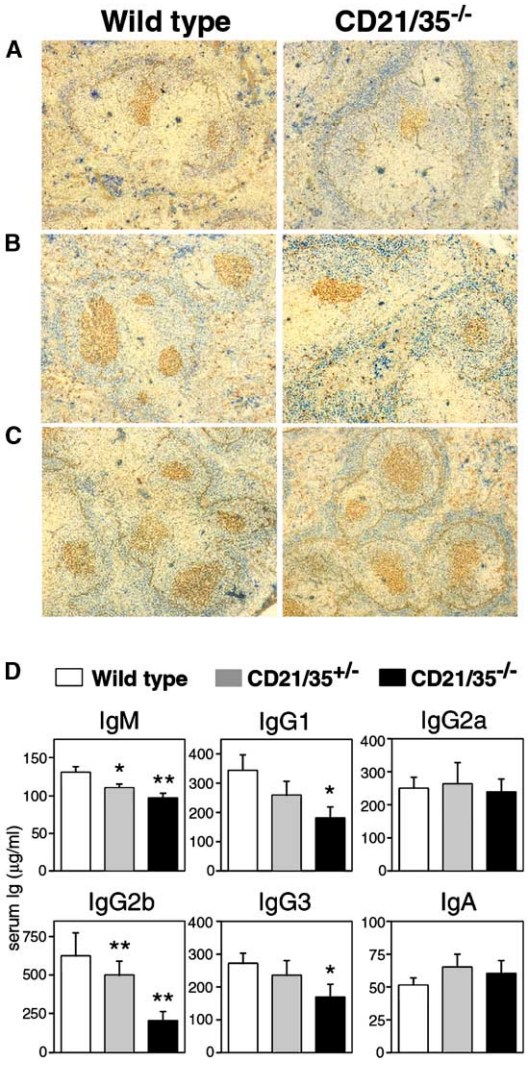

Figure 3. GC Formation and Serum Ig Levels in CD21/35$^{-/-}$ Mice

(A–C) Detection of PNA^{+}-GCs (brown) and IgM^{+} cells (blue) in spleens of naive CD21/35$^{-/-}$ and wild-type littermates (A) and during secondary responses (day 28) in mice immunized with 5×10^5 SRBC (B) or mice immunized with 10 μg DNP-KLH in alum (C).

(D) Serum Ig levels from ≥10 naive mice of each genotype at 2 months of age were determined by ELISA. Significant differences between means are indicated by asterisks. *, $p < 0.05$; **, $p < 0.01$.

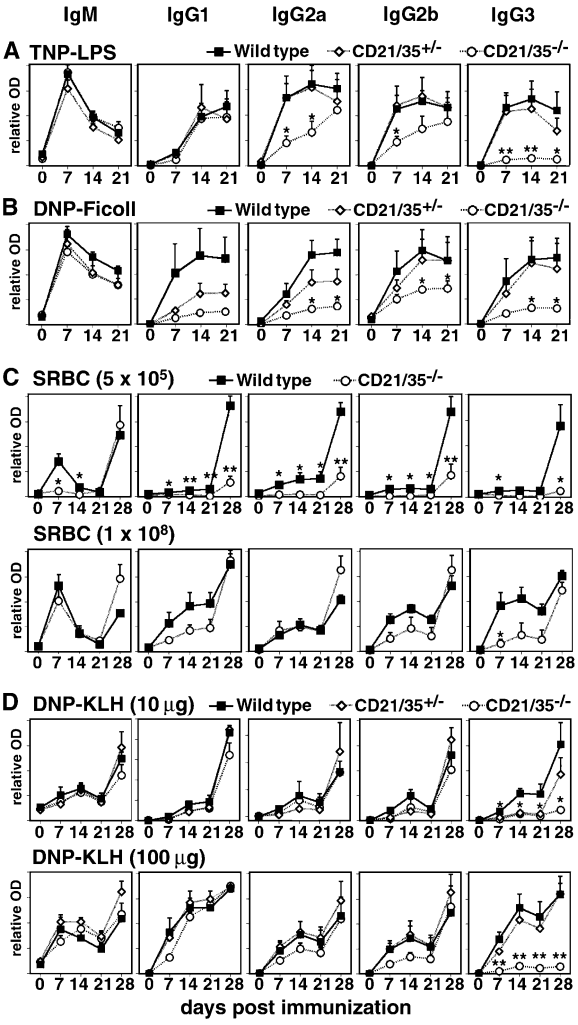

Figure 4. Antibody Responses of Wild-Type, CD21/35$^{+/-}$, and CD21/35$^{-/-}$ Littermates

Antibody responses following TNP-LPS (A) and DNP-Ficoll (B) immunization. Antibody responses following SRBC (C) and DNP-KLH in alum (D) immunization with rechallenge on day 21. Values represent mean OD_{405} results (± SEM) from individual mice as measured by antigen-specific ELISAs for groups of four to five mice of each genotype. Significant differences in means between CD21/35$^{-/-}$ and wild-type littermates are indicated by asterisks. *, $p < 0.05$; **, $p < 0.01$.

termates (438 ± 74 versus 2000 ± 495, respectively, $p < 0.05$; Figure 6A). Boosting with 10^5 heat-killed bacteria 14 days following primary immunization raised the antibody titers to equivalent levels on day 21 (Figure 6A), which correlated with protection from infection (Figure 5E). At this immunizing dose and these time points, the vast majority of WU-2-specific antibody detected was of the IgM isotype. However, immunizing and boosting mice with 10^7 heat-killed bacteria induced measurable IgG responses (Figure 6B). IgM and IgG2a antibody titers in CD21/35$^{-/-}$ mice were half those of wild-type littermates during the primary response, while all other IgG isotypes were undetectable in CD21/35$^{-/-}$ mice. Nonetheless, this response provided CD21/35$^{-/-}$ mice with adequate protection against a lethal dose challenge of 5000 cfu (Figure 5F). Seven days following a boost of 10^7 heat-killed bacteria on day 14, IgM, IgG1, IgG2a, and IgG2b titers were similar between CD21/35$^{-/-}$ and wild-type littermates. However, WU-2-specific IgG3 titers remained >12-fold lower in CD21/35$^{-/-}$ mice compared to wild-type littermates. Thus, although CD21/35$^{-/-}$ mice initially produced less antibody to *S. pneumoniae* than wild-type mice, increasing the antigen dose and/or the number of immunizations overcame the deficient antibody response and afforded protection against lethal challenge.

Discussion

An important role for CD21/35 during innate and adaptive immune responses was reflected in the dramatic

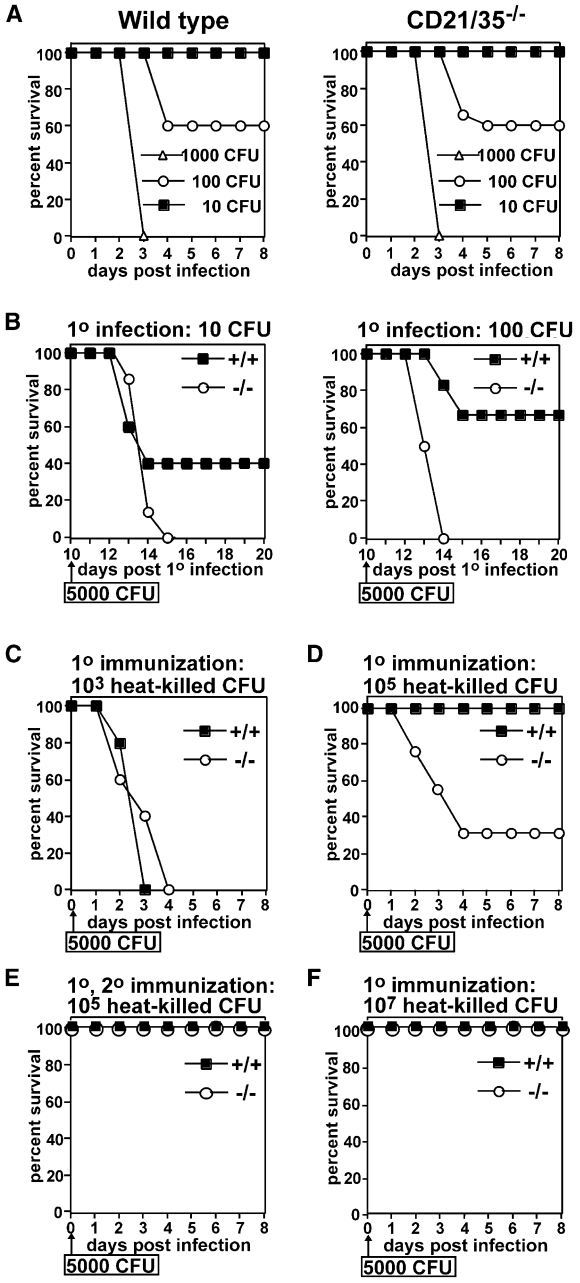

Figure 5. Survival of Wild-Type and CD21/35$^{-/-}$ Littermates following *S. pneumoniae* Challenge

(A) Survival of naive mice following infection with *S. pneumoniae*.
(B) Sublethal primary infection provides partial protection against a high-dose challenge in wild-type but not CD21/35$^{-/-}$ littermates. Ten days after the primary infection, mice were rechallenged with a lethal dose of bacteria (5000 cfu).
(C–E) Mice were immunized once with 10^3 (C), 10^5 (D), twice with 10^5 cfu at days 0 and 14 (E), or once with 10^7 (F) heat-killed cfu and challenged with 5000 cfu of live bacteria 10 (C, D, and F) or 7 (E) days later. Five to ten mice of each genotype were used for each challenge dose.

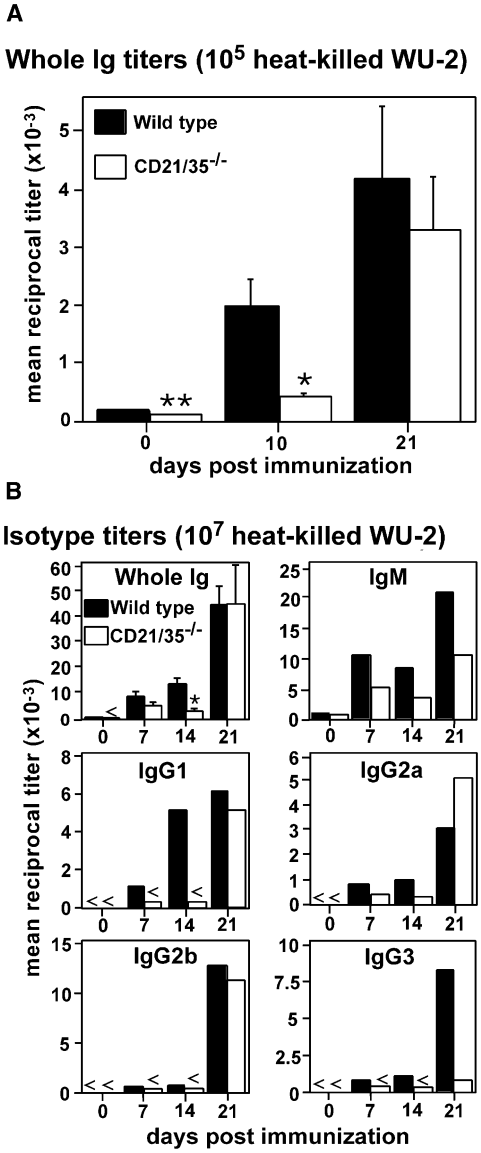

Figure 6. *S. pneumoniae*-Specific Serum Antibody Titers for Wild-Type and CD21/35$^{-/-}$ Littermates Immunized with Heat-Killed Bacteria

Mice were immunized with 10^5 (A) or 10^7 (B) heat-killed cfu WU-2 with a boost on day 14. Bacteria-specific antibody titers were determined by ELISA using 3-fold serial dilutions beginning at 1:100. Whole Ig titers were determined for serum samples from individual mice (A and B) while isotype-specific titers (B) were determined for pooled sera. Titers represent results from five to six mice/group with reciprocal titers $\leq$200 indicated ($<$). For whole Ig titers, values represent the mean titer ($\pm$ SEM) with significant differences between means indicated by asterisks. *, $p < 0.05$; **, $p < 0.01$.

susceptibility of CD21/35$^{-/-}$ mice to acute lethal *S. pneumoniae* infection, despite immunization. Although naive CD21/35$^{-/-}$ and wild-type littermates were equivalent in their susceptibility to acute challenge, CD21/35 expression significantly enhanced protective humoral immune responses to immunization or subsequent bacterial challenge. Complete protection of CD21/35$^{-/-}$ mice during bacterial challenge was achieved when mice were given either multiple immunizations or 100-fold higher doses of immunogenic heat-killed bacteria. These results indicate an impaired ability of low-concentration antigens to rapidly generate protective responses in CD21/35$^{-/-}$ mice, despite the intrinsic adju-

vanticity of intact bacteria. Since CD21/35 selectively targets antibody-antigen-C3d complexes to B cells and follicular dendritic cells (FDCs) (Fang et al., 1998; Wu et al., 2000), CD21/35 is likely to also selectively focus bacterial antigens to these cells during acute infections. Thereby, CD21/35 expression may facilitate the processing and presentation of antigens at low concentrations, particularly in the absence of preformed or natural antibodies where Fc receptor interactions may also facilitate immune complex processing (Thornton et al., 1994). Alternatively, intrinsic defects in B cell function may result from CD21/35 deficiency although B cells from CD21/35$^{-/-}$ mice (data not shown) function normally during in vitro assays. The impaired antibody responses of CD21/35$^{-/-}$ mice to TI and TD antigens may be due to the absence of one or more of these multifaceted functions, with the requirement for CD21/35 expression diminished when antigen or antigen-specific antibody concentrations exceed threshold levels.

CD21/35 functions as an important component of the innate immune system since CD21/35$^{-/-}$ mice were unable to focus C3d-bearing complexes to the marginal zones of splenic follicles or on the surface of B cells in vivo. Many TI and TD antigens activate complement via the alternative pathway or activate the classical pathway after binding natural antibodies reactive with pathogenic microorganisms (Griffioen et al., 1991; Pryjma et al., 1974). The covalent attachment of C3 cleavage products thereby provides a mechanism by which antigens can be directly targeted to complement receptor-expressing cells. Indeed, marginal zone B cells express high levels of CD21, and pneumococcal polysaccharides (PS) preferentially localize on marginal zone B cells and FDCs along with C3 (Peset Llopis et al., 1996). This may explain why conjugation of C3d to capsular PS augments TI antibody responses (Test et al., 2001). In the absence of C3 or with decreased levels of CD21/35 expression, marginal zone B cells do not bind TNP-Ficoll efficiently in vivo (Guinamard et al., 2000). In addition, poor responsiveness of neonates to TI-2 antigens is attributed to their insufficient CD21 expression and lack of marginal zone B cells (Timens et al., 1989). Thus, CD21/35 may regulate the production of TI antigen-elicited antibodies by targeting C3d-antigen complexes to marginal zone B cell populations, which are produced in normal to augmented numbers even when CD21/35 expression is reduced. Based on the high level of C3dg-tetramer binding observed for naive B cells in vivo, C3-tagged complexes may augment CD19 function and thereby enhance B cell transmembrane signaling in a large fraction of B cells. This indicates a critical role for CD21/35 not only in the rapid trapping of C3d-Ag-complexes in marginal zones but also in the localization of C3d-decorated antigen to B cells in a manner independent of their antigen receptor specificity.

A striking characteristic of CD21/35$^{-/-}$ mice was their inability to generate significant IgG3 antibody responses to TI, TD, and bacterial antigens compared with wild-type littermates. IgG3 is the major mouse IgG isotype produced in response to TI-2 antigens (Perlmutter et al., 1978). Mice unable to produce IgG3 in response to TI-2 antigens, such as *xid* and γ3 gene-disrupted mice, are more susceptible to pneumococcal infection as IgG3 anti-PS antibodies may be the major opsonin (Briles et al., 1986; McLay et al., 2002). In humans, IgG2 is the major IgG isotype produced in response to most TI antigens during late ontogeny (Shackelford et al., 1988). Human IgG2 deficiency is associated with increased susceptibility to chronic sinopulmonary infections, highlighting its importance in resistance to encapsulated bacteria (Kuijpers et al., 1992). Mouse IgG3 demonstrates superior binding to polysaccharide antigens which results in enhanced activation of effector function, including complement activation and Fc receptor binding (Greenspan and Cooper, 1993). Therefore, deficient IgG3 production by CD21/35$^{-/-}$ mice may be the primary explanation for their increased susceptibility to bacterial infection. Given the essential role of B cells in protection from encapsulated bacteria (Wardemann et al., 2002) and the importance of marginal zone and B1a B cell populations in IgG3 responses (Guinamard et al., 2000; Hardy et al., 1994), localization of C3d complexes to these B cell subsets may be central to the generation of protective antibody responses during acute infections.

The production of a third line of CD21/35$^{-/-}$ mice clarifies the functional and phenotypic characteristics of this genotype since one line was recently found to express a hypomorphic cell-surface CD21/35 protein at 30%–40% of wild-type levels (Hasegawa et al., 2001). The CD21/35^{hypo} protein retained its C3d binding region, and CD21/35^{hypo} mice mediated C3dg-tetramer binding at 30%–40% of wild-type levels. Nonetheless, all three lines of CD21/35$^{-/-}$ mice have typical frequencies and numbers of bone marrow and peripheral B cells. However, the new line of CD21/35$^{-/-}$ mice had a significant reduction in the size of the IgM^{lo}IgD^{hi} population in the spleen, while the IgM^{hi}IgD^{lo} population was expanded. Increased numbers of IgM^{hi}IgD^{lo} splenocytes in CD21/35$^{-/-}$ mice may be explained by an expanded marginal zone B cell population, as suggested in a previous study using CD21/35^{hypo} mice (Cariappa et al., 2001). The IgM^{hi}IgD^{lo} B cell expansion is unlikely to represent expansion of B1a cells, as CD5^{+} splenic B cell frequencies and peritoneal B1a cell numbers were normal in our CD21/35$^{-/-}$ mice, as reported previously for CD21/35-targeted mice (Molina et al., 1996). Thus, development of the B1a population proceeds normally in the absence of CD21/35 expression (Hasegawa et al., 2001) in contrast to previous reports (Ahearn et al., 1996). This finding contrasts with the impaired B1a cell development observed in CD19$^{-/-}$ mice (Rickert et al., 1995; Sato et al., 1996). That CD19 deficiency has a more significant effect on B cell function than CD21/35 deficiency is explained by CD19 function that is independent of CD21/35 expression (Hasegawa et al., 2001). Relative to previously described CD21/35-targeted mouse lines (Ahearn et al., 1996; Molina et al., 1996), CD21/35$^{-/-}$ mice described herein had reduced numbers of secondary follicles before immunization and following secondary antigen challenge, lower relative serum Ig levels with significantly reduced IgM levels, more impaired antibody production during primary and secondary responses to a low-dose TD antigen (SRBC), and significantly reduced IgG3 antibody responses following antigen challenge. Collectively, these results indicate a dual role for CD21/35 in innate and adaptive humoral responses.

In summary, the current studies reveal that CD21/

35 is a critical regulator of both TI and TD antibody responses, particularly in response to low-level antigen challenge. Furthermore, a unique role for CD21/35 in promoting IgG3 antibody responses was revealed. Undoubtedly, the role of CD21/35 in localization of blood-borne antigens on marginal zone B cells is central to these outcomes. Using model antigens, others have proposed that marginal zone B cell trapping of antigens has a critical role in host defense against bacterial pathogens since the proximity of marginal zone B cells to marginal sinuses ensures that they are among the first population of cells to encounter blood-borne antigens (Martin et al., 2001). Consistent with this, marginal zone B cells generate rapid activation, and proliferative and Ig secretory responses (Oliver et al., 1999). Thus, TI and TD bacterial antigens that activate complement are likely to become focused onto marginal zone B cells by virtue of their high-level CD21/35 receptor expression and proximal association with the splenic microvasculature. Thereby, CD21 crosslinking and its activation of the CD19 regulatory pathway would make B cells more responsive to transmembrane signals (Poe et al., 2001). This provides yet another molecular example of how the innate and adaptive immune responses cooperatively interact to hasten antigen recognition and enhance the generation of nascent humoral immune responses during life-threatening encounters with virulent pathogens.

Experimental Procedures

Generation of CD21/35$^{-/-}$ Mice

A 12 kb DNA fragment encoding the 5′ end of the mouse *Cr2* gene was isolated from a 129/SvJ genomic library, subcloned into pBluescript SK (Stratagene, La Jolla, CA), sequenced, and mapped for restriction endonuclease sites (Figure 1A). Two DNA fragments flanking the signal sequence were sequentially inserted into a pBluescript SK-based targeting vector (p594; provided by Dr. D. Milstone, Brigham and Women's Hospital, Boston, MA) containing the PGK promoter, neomycin resistance marker, and poly(A) signal sequence from pGK-neo poly(A) (Stratagene; Figure 1B). A 5.7 kb BstEII DNA fragment was blunt-inserted proximal to the HSV-tk gene (Figure 1B). A 1.3 kb HpaI-XbaI DNA fragment upstream of SCR1 formed the 3′ arm of the targeting vector. R1 ES cells were transfected with SalI-linearized plasmid DNA and selected for G418 resistance as described (Selfridge et al., 1992). Appropriately targeted ES cell clones were identified by Southern blot analysis of genomic DNA digested with BstXI using an 800 bp SpeI-XhoI probe. Targeted ES clones were then screened using a PCR strategy that amplified a region between the signal sequence and SCR1 of the *Cr2* locus external to the targeted vector. The PCR strategy used a 3′ primer outside of the targeted vector region in combination with either a neo-specific primer or an intron-specific primer as indicated in Figure 1C to yield 1.8 and 1 kb PCR products, respectively. Ten targeted ES clones were microinjected into 3.5-day-old C57BL/6J blastocysts, which were then implanted into pseudopregnant females. Two of six chimeric offspring from independent ES clones were crossed with C57BL/6J mice to generate offspring heterozygous for the disrupted *Cr2* allele. Offspring were screened by the PCR strategy described above and by Southern blot analysis of DNA extracted from tail tissue using BstEII digestion and a probe specific for the 5′ flanking sequence (BstEII-BamHI; Figure 1A). Mice heterozygous for the mutated allele were intercrossed to generate homozygous, heterozygous, and wild-type littermates for use in experiments.

CD21/35^{hypo} mice (Ahearn et al., 1996) were generously supplied by Dr. Michael Carroll (Center for Blood Research, Harvard Medical School, Boston, MA). Mice were confirmed homozygous for the neo-disrupted *Cr2* locus by Southern blot or PCR analysis of genomic tail DNA (Ahearn et al., 1996). All experiments were carried out using mice between 2–3 months of age housed under specific pathogen-free conditions, except during *S. pneumoniae* challenges in which mice between 2–4 months of age were transferred to a conventional animal facility prior to infection. All studies and procedures were approved by the Duke University Animal Care and Use Committee.

Antibodies and Immunoflourescence Analysis

Biotinylated- or fluorochrome-conjugated antibodies used in this study included: anti-CD21 (7E9, provided by Dr. T. Kinoshita, Osaka University, Japan; Kinoshita et al., 1988), anti-mouse IgM or IgD (Southern Biotechnology Associates, Inc., Birmingham, AL), anti-B220 (RA3-6B2, provided by Dr. R. Coffman, DNAX Research Institute, Palo Alto, CA), goat F(ab′)$_2$ anti-rat IgG (H+L) (Southern Biotechnology), and antibodies reactive with CD21 (7G6), CD19 (ID3), B220 (RA3-6B2), CD5 (53-7.3), CD11b (M1/70), and CD43 (S7; BD PharMingen, San Diego, CA). Phycoerythrin- and cychrome-conjugated streptavidin were from PharMingen. Leukocytes (0.5–1 $\times$ 10^6) were incubated with antibodies at 4°C for 25 min, washed, and analyzed using a FACScan flow cytometer (Becton Dickinson, San Jose, CA), with positive and negative cell populations determined using unreactive isotype-matched antibodies.

C3dg-Tetramer Staining

Biotinylated C3dg was produced in AD494(DE3)pLysS bacteria (Novagen, Madison, WI) using the pET11d-C3dg-BSP-BirA expression plasmid and purified as described (Henson et al., 2001). To form C3dg tetramers, 0.25 μg streptavidin-phycoerythrin (SA-PE) was added to 1 μg of biotinylated C3dg in 100 μl PBS for 45 min at room temperature. Cells were incubated with C3dg-tetramers on ice, washed, and analyzed by flow cytometry. An equal concentration of biotinylated chicken γ globulin (CGG) complexed with SA-PE was used as a negative control.

To form C3dg-tetramers to be used for injections, 20 μg biotinylated C3dg (or CGG as a control) was incubated with 20 μg SA-PE in 200 μl PBS at room temperature for 45 min. C3dg was treated with polymyxin B-agarose (Sigma, St. Louis, MO) prior to injection. Tetramers (200 μl) were injected into tail veins of mice with spleens harvested 30 min later. Images of spleen sections (5 μM) were captured at a fixed exposure time using an Optronics MagnaFire digital imaging system.

Immunizations and *S. pneumoniae* Infections

Two-month-old mice were immunized intraperitoneally (i.p.) with 10 or 100 μg of DNP-KLH (Calbiochem-Novabiochem Corp., La Jolla, CA) precipitated in alum and boosted 21 days later. SRBC immunization was by i.v. tail vein injection of 5 $\times$ 10^5 or 1 $\times$ 10^8 SRBCs in 200 μl of PBS, followed by a boost at day 21. Mice were also immunized i.p. with 25 μg of DNP-Ficoll (Solid Phase Sciences, San Rafael, CA) or 50 μg of TNP-LPS (Sigma) in PBS.

WU-2 strain *S. pneumoniae* was grown in Todd-Hewitt broth supplemented with 0.5% yeast extract and was frozen as glycerol stocks at −70°C. At the time of infection, bacteria were diluted in sterile PBS for i.p. injection, and the number of cfus injected was reconfirmed by enumerating colony growth on blood agar plates (BAP). Heat-killed WU-2 bacteria were generated by incubating bacteria at 60°C for 2 hr, with death confirmed by the absence of growth on BAP.

Enzyme-Linked Immunosorbent Assays (ELISAs)

Hapten-specific and SRBC ELISAs were performed as described previously (Hasegawa et al., 2001; Mori et al., 1989). For *S. pneumoniae*-specific antibody ELISAs, ELISA plates were coated with 100 μl of heat-killed WU-2 diluted to 4 $\times$ 10^7 cfu/ml in 0.1 M borate buffered saline and incubated overnight at 4°C. Endpoint titers of sera were determined using 3-fold serial dilutions and taken as the reciprocal dilution of serum yielding an OD_{405} value that was 3-fold higher than that of the negative control OD with sera omitted.

Immunohistochemistry

Serial (5 μm) frozen spleen sections mounted on gelatin-coated slides were fixed in acetone, rehydrated in PBS, blocked in 5% normal rabbit serum/2% bovine calf serum in PBS, and stained with HRP-conjugated peanut agglutinin (PNA, Sigma) followed by

detection with 3,3′-diaminobenzidine substrate (DAB, Vector Laboratories, Burlingame, CA) to visualize GCs. AP-conjugated goat anti-mouse IgM antibody (Southern Biotechnology) was used in conjunction with Vector blue AP substrate kits (Vector Laboratories) to detect follicles.

Western Blot Analysis

Splenic B cells were enriched by removing T cells with anti-Thy1.2 antibody-conjugated magnetic beads (Dynal Inc., Lake Success, NY) and lysed in 1% NP40 lysis buffer. Protein samples were resolved on a 6% denaturing SDS-PAGE gel and transferred to nitrocellulose. Following blocking, the membranes were incubated with goat anti-mouse CD21/35 polyclonal antisera (D-19 or M-19; Santa Cruz Biotechnology, Santa Cruz, CA), followed by incubation with donkey anti-goat IgG-HRP (Jackson Immunoresearch Laboratories, West Grove, PA) and detection by enhanced chemiluminescence (ECL kit, Pierce, Rockford, IL).

Statistical Analysis

Data are shown as mean values ± SEM. The Student's t test was used to determine whether there were significant differences between sample means. Fisher's exact test was used to analyze differences in survival between groups following *S. pneumoniae* infection.

Acknowledgments

We thank Dr. Lili Tu for help in the generation of the CD21/35 targeting vector, Janice King for assistance with the infection experiments, and Dr. Michael Carroll for providing CD21/35^{hypo} mice. These studies were supported by NIH grants CA54464, CA81776, and AI24158 and a grant from the Arthritis Foundation. K.M.H. was supported in part by a fellowship from the Lymphoma Research Foundation.

Received: July 29, 2002
Revised: October 9, 2002

References

Ahearn, J.M., Fischer, M.B., Croix, D., Goerg, S., Ma, M., Xia, J., Zhou, X., Howard, R.G., Rothstein, T.L., and Carroll, M.C. (1996). Disruption of the *Cr2* locus results in a reduction in B-1a cells and in an impaired B cell response to T-dependent antigen. Immunity *4*, 251–262.

Bitter-Suermann, D., and Burger, R. (1989). C3 deficiencies. Curr. Top. Microbiol. Immunol. *153*, 223–233.

Botto, M., and Walport, M.J. (1993). Hereditary deficiency of C3 in animals and humans. Int. Rev. Immunol. *10*, 37–50.

Briles, D.E., Benjamin, W.H., Jr., Huster, W.J., and Posey, B. (1986). Genetic approaches to the study of disease resistance: with special emphasis on the use of recombinant inbred mice. Curr. Top. Microbiol. Immunol. *124*, 21–35.

Brown, E.J., Hosea, S.W., and Frank, M.M. (1981). The role of complement in the localization of pneumococci in the splanchnic reticuloendothelial system during experimental bacteremia. J. Immunol. *126*, 2230–2235.

Burman, L.A., Norrby, R., and Trollfors, B. (1985). Invasive pneumococcal infections: incidence, predisposing factors, and prognosis. Rev. Infect. Dis. *7*, 133–142.

Cariappa, A., Tang, M., Parng, C., Nebelitskiy, E., Carroll, M., Georgopoulos, K., and Pillai, S. (2001). The follicular versus marginal zone B lymphocyte cell fate decision is regulated by Aiolos, Btk, and CD21. Immunity *14*, 603–615.

Chen, Z., Koralov, S.B., Gendelman, M., Carroll, M.C., and Kelsoe, G. (2000). Humoral immune responses in Cr2$^{-/-}$ mice: enhanced affinity maturation but impaired antibody persistence. J. Immunol. *164*, 4522–4532.

Circolo, A., Garnier, G., Fukuda, W., Wang, X., Hidvegi, T., Szalai, A.J., Briles, D.E., Volanakis, J.E., Wetsel, R.A., and Colten, H.R. (1999). Genetic disruption of the murine complement C3 promoter region generates deficient mice with extrahepatic expression of C3 mRNA. Immunopharmacology *42*, 135–149.

Fang, Y., Xu, C., Fu, Y.-X., Holers, V.M., and Molina, H. (1998). Expression of complement receptors 1 and 2 on follicular dendritic cells is necessary for the generation of a strong antigen-specific IgG response. J. Immunol. *160*, 5273–5279.

Fearon, D.T., and Carroll, M.C. (2000). Regulation of B lymphocyte responses to foreign and self-antigens by the CD19/CD21 complex. Annu. Rev. Immunol. *18*, 393–422.

Figueroa, J.E., and Densen, P. (1991). Infectious diseases associated with complement deficiencies. Clin. Microbiol. Rev. *4*, 359–395.

Fischer, M.B., Ma, M., Goerg, S., Zhou, X., Xia, J., Finco, O., Han, S., Kelsoe, G., Howard, R.G., Rothstein, T.L., et al. (1996). Regulation of the B cell response to T-dependent antigens by classical pathway complement. J. Immunol. *157*, 549–556.

Greenspan, N.S., and Cooper, L.J. (1993). Cooperative binding by mouse IgG3 antibodies: implications for functional affinity, effector function, and isotype restriction. Springer Semin. Immunopathol. *15*, 275–291.

Griffioen, A.W., Rijkers, G.T., Janssens-Korpela, P., and Zegers, B.J. (1991). Pneumococcal polysaccharides complexed with C3d bind to human B lymphocytes via complement receptor type 2. Infect. Immun. *59*, 1839–1845.

Guinamard, R., Okigaki, M., Schlessinger, J., and Ravetch, J.V. (2000). Absence of marginal zone B cells in Pyk-2-deficient mice defines their role in the humoral responses. Nat. Immunol. *1*, 31–36.

Hardy, R.R., Carmack, C.E., Li, Y.S., and Hayakawa, K. (1994). Distinctive developmental origins and specificities of murine CD5^{+} B cells. Immunol. Rev. *137*, 91–118.

Hasegawa, M., Fujimoto, M., Poe, J.C., Steeber, D.A., and Tedder, T.F. (2001). CD19 can regulate B lymphocyte signal transduction independent of complement activation. J. Immunol. *167*, 3190–3200.

Hebell, T., Ahearn, J.M., and Fearon, D.T. (1991). Suppression of the immune response by a soluble complement receptor of B lymphocytes. Science *254*, 102–105.

Henson, S.E., Smith, D., Boackle, S.A., Holers, V.M., and Karp, D.R. (2001). Generation of recombinant human C3dg tetramers for the analysis of CD21 binding and function. J. Immunol. Methods *258*, 97–109.

Heyman, B., Wiersma, E.J., and Kinoshita, T. (1990). In vivo inhibition of the antibody response to a complement receptor-specific monoclonal antibody. J. Exp. Med. *172*, 665–668.

Kinoshita, T., Takeda, J., Hong, K., Kozono, H., Sakai, H., and Inoue, K. (1988). Monoclonal antibodies to mouse complement receptor type 1 (CR1). Their use in a distribution study showing that mouse erythrocytes and platelets are CR1-negative. J. Immunol. *140*, 3066–3073.

Kuijpers, T.W., Weening, R.S., and Out, T.A. (1992). IgG subclass deficiencies and recurrent pyogenic infections: unresponsiveness against bacterial polysaccharide antigens. Allergol. Immunopathol. *20*, 28–34.

Loder, F., Mutschler, B., Ray, R.J., Paige, C.J., Sideras, P., Torres, R., Lamers, M.C., and Carsetti, R. (1999). B cell development in the spleen takes place in discrete steps and is determined by the quality of B cell receptor-derived signals. J. Exp. Med. *190*, 75–89.

Martin, F., Oliver, A.M., and Kearney, J.F. (2001). Marginal zone and B1 B cells unite in the early response against T-independent blood-borne particulate antigens. Immunity *14*, 617–629.

McLay, J., Leonard, E., Petersen, S., Shapiro, D., Greenspan, N.S., and Schreiber, J.R. (2002). Gamma-3 gene-disrupted mice selectively deficient in the dominant IgG subclass made to bacterial polysaccharides. II. Increased susceptibility to fatal pneumococcal sepsis due to absence of anti-polysaccharide IgG3 is corrected by induction of anti-polysaccharide IgG1. J. Immunol. *168*, 3437–3443.

Molina, H., Holers, V.M., Li, B., Fang, Y.-F., Mariathasan, S., Goellner, J., Strauss-Schoenberger, J., Karr, R.W., and Chaplin, D.D. (1996). Markedly impaired humoral immune response in mice deficient in complement receptors 1 and 2. Proc. Natl. Acad. Sci. USA *93*, 3357–3361.

Mori, H., Sakamoto, O., Xu, Q.A., Daikoku, M., and Koda, A. (1989). Solid phase enzyme-linked immunosorbent assay (ELISA) for anti-sheep erythrocyte antibody in mouse serum. Int. J. Immunopharmacol. *11*, 597–606.

Ochsenbein, A.F., Pinschewer, D.D., Odermatt, B., Carroll, M.C., Hengartner, H., and Zinkernagel, R.M. (1999). Protective T cell-independent antiviral antibody responses are dependent on complement. J. Exp. Med. *190*, 1165–1174.

Oliver, A.M., Martin, F., and Kearney, J.F. (1999). $IgM^{high}CD21^{high}$ lymphocytes enriched in the splenic marginal zone generate effector cells more rapidly than the bulk of follicular B cells. J. Immunol. *162*, 7198–7207.

Pepys, M.B. (1974). Role of complement in induction of antibody production in vivo. Effect of cobra venom factor and other C3-reactive agents on thymus-dependent and thymus-independent antibody responses. J. Exp. Med. *140*, 126–145.

Perlmutter, R.M., Hansburg, D., Briles, D.E., Nicolotti, R.A., and Davie, J.M. (1978). Subclass restriction of murine anti-carbohydrate antibodies. J. Immunol. *121*, 566–572.

Peset Llopis, M.J., Harms, G., Hardonk, M.J., and Timens, W. (1996). Human immune response to pneumococcal polysaccharides: complement-mediated localization preferentially on CD21-positive splenic marginal zone B cells and follicular dendritic cells. J. Allergy Clin. Immunol. *97*, 1015–1024.

Poe, J.C., Hasegawa, M., and Tedder, T.F. (2001). CD19, CD21 and CD22: multifaceted response regulators of B lymphocyte signal transduction. Int. Rev. Immunol. *20*, 739–762.

Pryjma, J., Humphrey, J.H., and Klaus, G.G. (1974). C3 activation and T-independent B cell stimulation. Nature *252*, 505–506.

Rickert, R.C., Rajewsky, K., and Roes, J. (1995). Impairment of T-cell-dependent B-cell responses and B-1 cell development in CD19-deficient mice. Nature *376*, 352–355.

Sato, S., Ono, N., Steeber, D.A., Pisetsky, D.S., and Tedder, T.F. (1996). CD19 regulates B lymphocyte signaling thresholds critical for the development of B-1 lineage cells and autoimmunity. J. Immunol. *157*, 4371–4378.

Selfridge, J., Pow, A.M., McWhir, J., Magin, T.M., and Melton, D.W. (1992). Gene targeting using a mouse HPRT minigene/HPRT-deficient embryonic stem cell system: inactivation of the mouse ERCC-1 gene. Somat. Cell Molec. Genet. *18*, 325–336.

Shackelford, P.G., Nelson, S.J., Palma, A.T., and Nahm, M.H. (1988). Human antibodies to group A streptococcal carbohydrate. Ontogeny, subclass restriction, and clonal diversity. J. Immunol. *140*, 3200–3205.

Test, S.T., Mitsuyoshi, J., Connolly, C.C., and Lucas, A.H. (2001). Increased immunogenicity and induction of class switching by conjugation of complement C3d to pneumococcal serotype 14 capsular polysaccharide. Infect. Immun. *69*, 3031–3040.

Thornton, B.P., Vetvicka, V., and Ross, G.D. (1994). Natural antibody and complement-mediated antigen processing and presentation by B lymphocytes. J. Immunol. *152*, 1727–1737.

Thyphronitis, G., Kinoshita, T., Inoue, K., Schweinle, J.E., Tsokos, G.C., Metcalf, E.S., Finkelman, F.D., and Balow, J.E. (1991). Modulation of mouse complement receptors 1 and 2 suppress antibody responses in vivo. J. Immunol. *147*, 224–230.

Timens, W., Boes, A., Rozeboom-Uiterwijk, T., and Poppema, S. (1989). Immaturity of the human splenic marginal zone in infancy. Possible contribution to the deficient infant immune response. J. Immunol. *143*, 3200–3206.

Wardemann, H., Boehm, T., Dear, N., and Carsetti, R. (2002). B-1a B cells that link the innate and adaptive immune responses are lacking in the absence of the spleen. J. Exp. Med. *195*, 771–780.

Wessels, M.R., Butko, P., Ma, M., Warren, H.B., Lage, A., and Carroll, M.C. (1995). Studies of group B streptococcal infection in mice deficient in complement C3 or C4 demonstrate an essential role for complement in both innate and acquired immunity. Proc. Natl. Acad. Sci. USA *92*, 11490–11494.

Winkelstein, J.A. (1981). The role of complement in the host's defense against *Streptococcus pneumoniae*. Rev. Infect. Dis. *3*, 289–298.

Wu, X., Jiang, N., Fang, Y., Xu, C., Mao, D., Singh, J., Fu, Y., and Molina, H. (2000). Impaired affinity maturation in $Cr2^{-/-}$ mice is rescued by adjuvants without improvement in germinal center development. J. Immunol. *165*, 3119–3127.